

Terahertz Spectroscopy of Emerging Materials

Jacob A. Spies,* Jens Neu, Uriel T. Tayvah, Matt D. Capobianco, Brian Pattengale, Sarah Ostresh, and Charles A. Schmuttenmaer

Cite This: *J. Phys. Chem. C* 2020, 124, 22335–22346

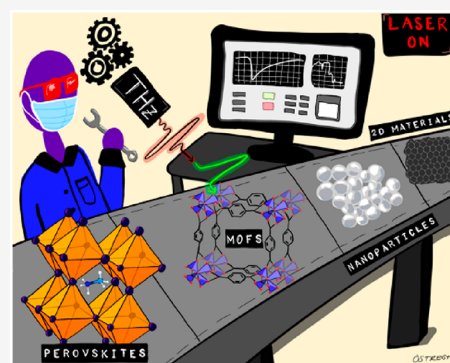
Read Online

ACCESS |

Metrics & More

Article Recommendations

ABSTRACT: Over the past few decades, terahertz (THz) spectroscopy has become an established technique for studying the dielectric and transient photoconductive properties of materials. THz spectroscopy is a contact-free probe of electrical conductivity with subpicosecond time resolution, and it has proven especially useful for studying emerging materials. We highlight recent work used to study metal halide perovskites, metal oxides, metal–organic frameworks, and 2D materials in addition to providing an overview of methods in pump–probe THz spectroscopy. We focus on the ways in which THz spectroscopy can be used to study charge transport mechanisms and factors that might limit carrier mobility in emerging materials. This Perspective will provide a general understanding of pump–probe THz spectroscopy and how it can be applied to next-generation materials and will identify challenges and advantages in data processing to extract broadband complex conductivity spectra.



INTRODUCTION

Materials science is ubiquitous in our everyday lives, ranging from carbon fiber reinforced polymer tennis rackets and Formula 1 chassis, to hip joint prostheses, and to the photovoltaics that are expected to fully power our society in the future. In the case of the latter, the development of materials with applications in energy conversion and storage are paramount scientific challenges. During the development of new materials, characterization is an important step in benchmarking performance and understanding why a device performs as it does. Although there are many existing characterization techniques, those that analyze electrical properties are especially useful in energy conversion.

In the past century, dozens of different techniques to determine electrical properties have been developed, ranging from simple two-point DC measurements to Hall effect measurements.¹ However, most of these contact-based techniques require the fabrication of electrical contacts on the materials. This is particularly challenging for emerging materials because the sample needs to be sufficiently large, homogeneous, and stable to allow the fabrication of electrical contacts. Furthermore, these fabrication techniques are time consuming, can alter the material itself, and are prone to disturbing the intrinsic properties of the material studied. These techniques also inherently probe long-distance conductivity phenomena spanning the distance between the probes, which include grain boundaries and defects. Therefore, they cannot effectively probe conductivity on the nanoscale, which is pertinent to many devices based on emerging materials.

In contrast with contact-based techniques, THz spectroscopy is a free-space optical technique that enables the investigation of

electro-optical properties of materials, including nanomaterials, directly in their native form.^{2–4} It is a contact-free electrical probe with subpicosecond temporal resolution and can be used in conjunction with material morphologies that range from large-scale single crystals to polycrystalline 2D nanoflakes and even amorphous materials. This makes THz spectroscopy a versatile and flexible technique to explore, understand, and benchmark (photo)conductivity in emerging materials, allowing for a rapid evaluation of a material's potential for photoelectrical applications. Furthermore, although THz was once only accessible to laboratories with significant laser optics expertise, it has become mainstream enough that commercial THz spectrometers have been on the market for a number of years, recently including more complex pump–probe systems, making it accessible to new users.

A PRACTICAL COURSE IN THz SPECTROSCOPY

In this section, we will introduce some of the advantages of THz spectroscopy and describe how a THz experiment is performed (Figure 1). Building on this, we will discuss different methods of THz generation and detection that may be encountered in the literature with an eye toward comparing their bandwidths and the different physical phenomena that can be observed within

Received: July 10, 2020

Revised: August 20, 2020

Published: September 11, 2020



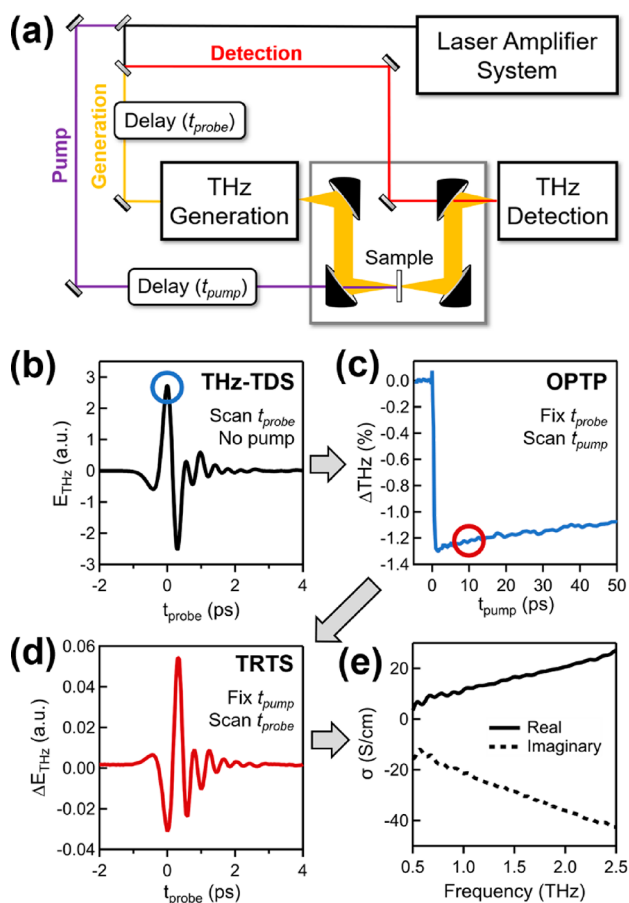


Figure 1. (a) Schematic diagram of a pump–probe THz spectrometer showing the three beam paths and time delays (t_{probe} and t_{pump}). (b) Reference THz waveform measured by THz time-domain spectroscopy (THz-TDS). (c) Optical-pump THz-probe (OPTP) measurement where t_{probe} is fixed at 0 ps (peak of reference waveform, denoted with a blue circle in panel b) and t_{pump} is scanned. (d) Time-resolved THz spectroscopy (TRTS) measurement where the differential THz waveform is measured (t_{probe} is scanned) at a fixed t_{pump} (e.g., red circle in panel c) and (e) resulting complex conductivity spectrum calculated numerically using Fourier transformation, the differential THz waveform, and a reference.² Gray arrows show the typical workflow to collect a photoconductivity spectrum. Scans and spectrum were adapted from Si nanoparticles embedded in Nafion, as previously reported in ref 6. Copyright 2020 American Chemical Society.

that bandwidth (Figure 2). Finally, with a knowledge of the manner in which a THz experiment is performed and what physical phenomena may be measured, we will discuss data analysis, comparing simplified approximative processing with more advanced but somewhat computationally demanding approaches. The goal of this section is three-fold: to familiarize the reader with THz spectroscopy, to demonstrate how THz spectroscopy is useful in materials science research, and to provide an overview of the capabilities of state-of-the-art methods in table-top THz spectroscopy and data analysis.

Anatomy of a THz Experiment. Figure 1a shows a schematic of a typical pump–probe THz spectrometer based on an amplified laser system, such as the commonly used Ti:sapphire system. The output of the amplifier is split into three beams for THz generation, THz detection, and optical photoexcitation. As is the case with any ultrafast pump–probe experiment, the time delays are controlled by mechanical delay stages, setting the THz probe time delay (t_{probe}) and the optical

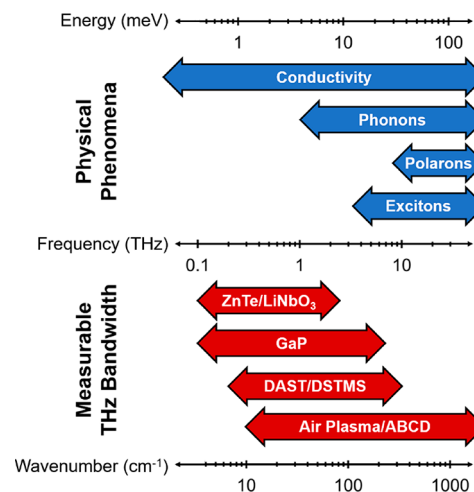


Figure 2. (Top) Examples of physical phenomena relevant to the charge transport and performance of emerging materials that appear in the THz regime and are discussed herein. (Bottom) Comparison of bandwidths achievable using various THz generation and detection methods. DAST, DSTMS = organic THz electro-optic crystals; ABCD = air-biased coherent detection.

photoexcitation time delay (t_{pump}) relative to the detection beam timing. It is important to note that t_{probe} is placed in the generation line, which ensures that every point in the differential THz field measured experiences the same delay from the visible photoexcitation (t_{pump}).⁵ This is important for frequency-dependent measurements because it removes the photoexcited timing ambiguity from the differential THz waveform.

With this spectrometer, three distinct types of THz measurements can be performed, depending on which delay lines are scanned (and if there is optical photoexcitation):

(1) In a THz time-domain spectroscopy (THz-TDS) experiment, there is no photoexcitation, and only t_{probe} is scanned to measure the transmitted THz waveform (Figure 1b). THz-TDS can be thought of as “steady-state” THz spectroscopy, analogous to standard FTIR spectroscopy. That is, whereas the data are collected in the time domain, the experiments are not time-resolved. However, in contrast with FTIR, THz-TDS also extracts the frequency-dependent phase in addition to the magnitude, thereby allowing complex-valued optical parameters to be extracted unambiguously.² These measurements are used as a reference to accurately process the photoexcited measurements.

(2) In an optical-pump THz probe (OPTP) experiment, t_{probe} is fixed at the maximum amplitude of the transmitted THz waveform (blue circle in Figure 1b), and the change in this amplitude is measured while scanning t_{pump} (Figure 1c). By definition, the maximum of the peak amplitude occurs when all of the spectral components are in-phase with each other. Thus the change in peak amplitude as a function of t_{pump} is proportional to the change in the conductivity of the sample, as probed with the full bandwidth of the spectrometer, and allows one to extract the free carrier kinetics in the system. For example, a decrease in broadband transmission would result from the formation of free carriers (e.g., charge injection), and the subsequent recovery back toward the baseline would result from carrier trapping or recombination. These measurements have subpicosecond time resolution and a time range of a few nanoseconds, limited by the length of the mechanical pump delay stage for t_{pump} . However, this time range can be extended

using electronic synchronization and delays to perform suprananosecond measurements.⁷

(3) Finally, in a *time-resolved THz spectroscopy* (TRTS) experiment, t_{pump} is fixed at the time of interest, and t_{probe} is scanned to measure the differential THz waveform at a particular time after photoexcitation (Figure 1d). Using the differential trace and a reference scan, the photoexcited and non-photoexcited traces are determined. These traces can then be Fourier-transformed to yield the frequency-dependent THz transmission. This is directly linked to the change in the complex refractive index, which is calculated from the transmission spectra, as discussed later.^{2,8} In many materials, the change upon photoexcitation is caused solely by a change in conductivity. However, transmission changes can also result from other phenomena such as nonlinear or resonant effects⁹ or a change in the permittivity of the material upon photoexcitation,¹⁰ so care must be taken when analyzing the data.

It is important to note that the OPTP and TRTS naming convention and others are used ambiguously in the field. In the description above, we have used the most common convention. However, we caution the reader to be aware of this ambiguity when perusing the literature.

Physical Properties in the THz Regime. In the THz spectral range, there are two main effects that contribute to the interaction with the incident wave: high-frequency conductivity associated with free charges (electrons and/or holes) and dielectric effects caused by bound charges.^{2,11} It is important to note that whereas these phenomena are accessible in other spectral regions (e.g., conductivity can be also observed in the microwave regime, and polarization effects are more commonly associated with the mid-infrared), THz provides specific advantages. Broadly, phonons (e.g., large-scale lattice vibrations), polarons, and excitons, can all be found in the THz regime (Figure 2), giving THz spectroscopy access to these important phenomena. THz spectroscopy also has specific advantages in the study of charge transport. High-frequency conductivity is the phenomenon most commonly probed in pump–probe THz spectroscopy and can provide insight into the mobility of a material and carrier scattering processes. These scattering effects happen on a time scale of femtoseconds to picoseconds, which places them within the THz range in the frequency domain. More broadly, THz spectroscopy is unique in providing simultaneous access to both high-frequency conductivity information and low-energy polarization effects. In the solid-state materials discussed herein, the high-frequency conductivity and a handful of resonant features are the most useful for understanding charge transport phenomena. In particular, electron–phonon interactions often reveal intrinsic factors that limit the mobility and charge transport in an emerging material. At room temperature, phonon modes in the THz regime are thermally populated ($298\text{ K} = 25.7\text{ meV} = 6.2\text{ THz}$), meaning that electron–phonon interactions in the THz regime can have a significant effect on even the DC conductivity.

Three processes commonly dominate intrinsic mobility: particle–particle scattering, electron–phonon interactions such as polaron formation, and exciton formation. These factors are intrinsic to the material, as opposed to extrinsic factors such as grain size. To rationally improve the performance of a material, it is important to know which of these phenomena are at play, and THz spectroscopy is well-suited for this pursuit. Polarons are formed when atoms surrounding a free carrier are displaced due to electrostatic attraction to the carrier. This interaction then creates a potential well around the carrier,

limiting its mobility. Because the formation of a polaron requires the distortion of the lattice, it often results in a signature in the phonon spectrum, which often lies in the THz regime. In addition to forming polarons, carriers can also form excitons: hydrogen-atom-like systems in which electrons are bound to holes and do not contribute to the measured conductivity. Here, too, THz spectroscopy is useful because this binding interaction is significantly screened, and exciton transitions often lie in the THz regime.¹²

While the observation of polarons, excitons, and other electron–phonon interactions is useful in its own right, the full strength of THz spectroscopy lies in its ability to weave these phenomena into a comprehensive picture of charge transport. In some cases, transient THz photoconductivity spectra can fit to a general photoconductivity model overlaid with more specific features (e.g., resonances from phonons or excitons). In such cases, the photoconductivity yields the broad strokes of charge transport while the specific features fill in more granular details.

However, measuring interesting physical phenomena requires an instrument with both sufficient spectral bandwidth and a high enough signal-to-noise ratio (SNR). Both the bandwidth and SNR are determined in large part by the THz generation and detection methods used. Here we discuss the performance of some of the most common methods used in THz spectroscopy, focusing on the trade-offs between these two parameters. In general, solid-state generation and detection provide higher nonlinear coefficients and therefore stronger fields, but the challenge of fulfilling phase-matching criteria results in a reduced bandwidth compared with air-based generation and detection.

The most commonly utilized solid-state generation and detection techniques used with amplifier-based systems are optical rectification (OR) and electro-optical sampling (EOS), respectively. OR is the difference-frequency analogue of second-harmonic generation, and EOS is based on the Pockels effect. OR and EOS are the most simply implemented and robust forms of THz generation and detection. These methods combine reasonable bandwidth with a good nonlinear conversion efficiency, allowing for a nonspecialized THz system that is easy to setup.

ZnTe and GaP are the most popular choices, with ZnTe having a large nonlinear coefficient and phase matching at 800 nm (resulting in higher SNR) and GaP having greater usable bandwidth ($\sim 0.1\text{--}7\text{ THz}$ versus $\sim 0.1\text{--}3\text{ THz}$; see Figure 2) due to the phonon mode being at a higher frequency and a lower cost.^{2,13} Additionally, LiNbO₃ is sometimes used to generate high-field THz for measuring THz nonlinearities or as a THz pump source, although is not as common due to the complicated tilted-pulse-front pumping geometry required to satisfy phase-matching conditions and the relatively narrow bandwidth (~ 0.1 to 2 THz).²

The current state-of-the-art in OR (and EOS) is the use of organic crystals such as DAST (4-*N,N*-dimethylamino-4'-*N'*-methyl-stilbazolium tosylate) and DSTMS (4-*N,N*-dimethylamino-4'-*N'*-methyl-stilbazolium 2,4,6-trimethylbenzenesulfonate). With their impressive bandwidth ($\sim 0.2\text{--}10\text{+ THz}$) and high field strengths,^{2,14,15} these organic crystals have enabled a wide variety of new THz measurements, such as 2D THz spectroscopy (i.e., THz-pump THz-probe).¹⁶ In contrast with the aforementioned methods, they often must be pumped in the near-infrared (1200–1700 nm) and have questionable reliability.

Air-based systems allow ultrabroadband “multi-THz” spectroscopy to be performed, utilizing a combination of air plasma

generation and air-biased coherent detection (ABCD), which commonly yield bandwidths in the range of 0.3–30+ THz (Figure 2).¹⁷ Although air plasma generation is fairly straightforward and cost-effective to implement, ABCD is much more challenging to construct and requires high voltages (tens of kilovolts).¹⁷ Therefore, many spectrometers utilizing air plasma generation as the THz source still employ EOS for detection.

Photoconductive antennae are commonly used for both generation and detection in oscillator-based THz-TDS systems and can also be used for THz detection on amplifier-based systems if care is taken to adjust the power of the laser beam within the limits of the antennae. For generation, an external bias is applied to a photoconductive switch, and the ultrafast current upon laser excitation emits THz radiation. The inverted effect can be used to detect THz electrical fields on the switch. Other less common sources are based on ultrafast (local) currents. For example, ultrafast spin currents and spin-selective scattering in thin magnetic/nonmagnetic metal layers emit THz radiation (called spintronic emitters).¹⁸

Introduction to THz Data Analysis. THz-TDS and TRTS directly measure the sign and magnitude of the transient electric field with femtosecond resolution, which upon Fourier transformation yields a complex-valued THz spectrum. This means that in addition to the intensity spectrum, the phase of the electromagnetic wave is also detected. This provides an important advantage as it allows one to determine the complex refractive index (and therefore the complex conductivity) spectrum.

In general, there are two commonly used approaches to ascertain the complex conductivity spectrum from TRTS measurements. The first is based on the so-called “thin-film approximation”. This approximation was originally applied to thin (~ 2 nm) superconducting films on a quartz substrate, and the core of this approximation is that the photoexcited film thickness is “thin”.¹⁹ The second common method involves transfer matrices and equations that can be defined based on the known sample geometry. The transfer function gives the change in amplitude and phase experienced by the pulse as it passes through the sample. This can be calculated in a straightforward way from the complex refractive indices of the layers making up the sample. These equations are then solved numerically for the complex refractive index for each frequency of interest, commonly in equally spaced small-frequency steps. For a more detailed description of this methodology, we refer the interested reader to work from our group by Neu et al.^{2,8} as well as a free software implementation downloadable online.²⁰

Both methods have their advantages and shortcomings.⁸ One advantage of the thin-film approximation is that it analytically relates the transmission to the conductivity by the following equation where σ is the complex conductivity, n is the nonphotoexcited refractive index of the substrate material, d is the photoexcited thickness, Z_0 is the impedance of free space (376.7Ω), and T is the transmission function, which is defined as $T(\omega, t_{\text{pump}}) = E_{\text{photo}}(\omega, t_{\text{pump}})/E_{\text{ref}}(\omega, t_{\text{pump}})$, where E_{photo} and E_{ref} are the complex transmission spectra for the photoexcited sample and nonphotoexcited reference.¹⁹

$$\sigma(\omega, t_{\text{pump}}) = \frac{n(\omega) + 1}{Z_0 d} \left(\frac{1}{T(\omega, t_{\text{pump}})} - 1 \right) \quad (1)$$

However, the usage of this approximation introduces two main challenges, the first being how thick can “thin” really be,⁸ and the

second relating to the introduction of artifacts when resonant features are present.⁹

To circumvent this challenge and determine the photo-induced change in the complex refractive index without invoking any models, it is necessary to use the transfer function approach. Here the photoinduced change can be calculated based on the static parameters and the known geometry.^{2,8} The static parameters of each layer need to be accurately known and are obtained by THz-TDS measurements of the sample material and the substrates. The calculation itself is slightly more computationally intense, requiring an optimization procedure at each frequency point of interest (instead of mere arithmetic, as with the thin-film approximation). However, an entire spectrum can be calculated in less than one minute on a moderate desktop or laptop computer (i.e., extensive computational resources are not required).

The photoconductivity spectrum is then used to gain insight into the underlying physical mechanisms that influence the conductivity. Depending on the material, several physically motivated or phenomenological models can be considered to describe the conductivity spectrum.²¹ The most common model is the Drude model. The basic assumption of this model is that the conductivity is due to free charges, which can be described as an electron gas. This assumption is valid for bulk, single-crystal materials such as GaAs. However, most emerging materials do not fulfill these criteria, and additional mechanisms need to be considered to accurately describe them. A common extension to the Drude model was proposed by Smith, resulting in the so-called “Drude–Smith” model, where σ_{DS} is the Drude–Smith conductivity, σ_0 is the static conductivity such that $\sigma_0 = Ne^2\tau/m^*$, N is the carrier density, e is the fundamental unit of charge, τ is the scattering time, and m^* is the effective electron mass.²²

$$\sigma_{\text{DS}}(\omega) = \frac{\sigma_0}{1 - i\omega\tau} \left(1 + \frac{c}{1 - i\omega\tau} \right) \quad (2)$$

The “persistence of velocity” parameter, or “ c -parameter”, can have values between 0 (which corresponds to the Drude model) and -1 . Values close to -1 significantly hinder long-range DC charge transfer and result in a low conductivity. This parameter was introduced as a phenomenological modification of the Drude model. However, several publications strongly suggest that this parameter is related to long-range charge transfer across grain or particle boundaries. These assumptions are also supported by recent work of Cocker et al.²³

The previous models describe only free charges. However, phonons, plasmons, excitons, and the effects of bound charges can be detected in the photoconductivity spectrum. These phenomena commonly exhibit resonant behavior, which can be described using the Lorentzian oscillator model. This additional term is commonly added to the conductivity model, such as the aforementioned Drude–Smith model.²⁴

■ THz SPECTROSCOPY IN MATERIALS SCIENCE

Perovskite Solar Absorbers. Metal halide perovskites are a class of semiconductor light absorbers that have garnered great interest over the past decade due to their strong solar absorption, long recombination lifetime, and high carrier mobility.⁵ THz spectroscopy has provided significant insights into this exciting class of materials and continues to provide new insight into understanding charge transport in perovskites. Such studies highlight how THz spectroscopy may be applied to other classes of emerging materials.

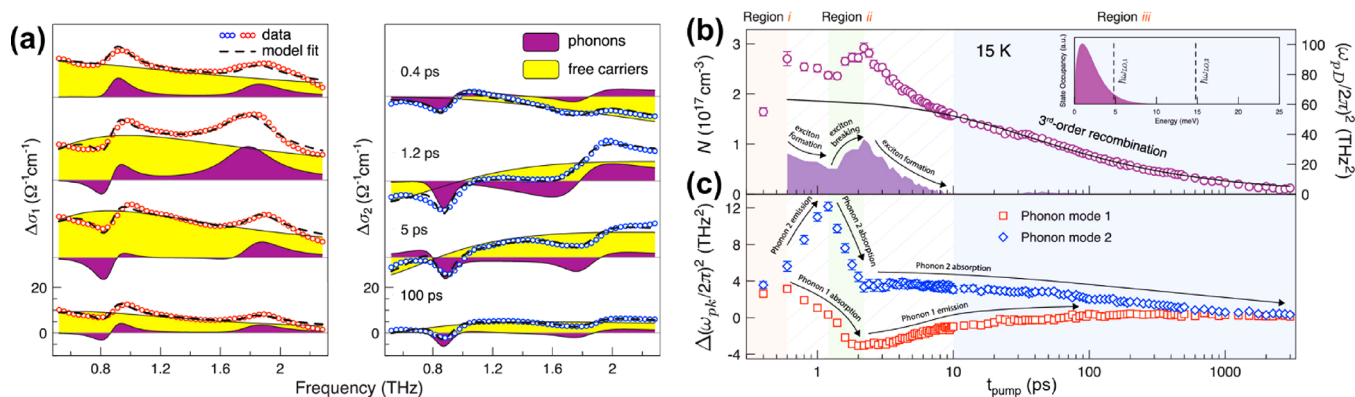


Figure 3. (a) Real ($\Delta\sigma_1$) and imaginary ($\Delta\sigma_2$) photoconductivity spectra at various pump–probe delays (t_{pump}). (b) Carrier density (N) and proportionally related Drude plasmon frequency (ω_{pD}) as a function of t_{pump} , showing theoretical third-order recombination (black line) and deviation attributed to exciton formation and breaking. (c) Phonon spectral weight ($\Delta(\omega_{\text{pk}}/2\pi)^2$) of both measured phonon modes as a function of t_{pump} showing phonon absorption and emission. All measurements were collected at 15 K. Adapted with permission from ref 24. Copyright 2019 American Chemical Society.

THz spectroscopy ultimately helps to measure carrier mobility and identify the factors that may limit carrier mobility. In perovskites, the carrier mobility should be similar to that of traditional inorganic ionic semiconductors such as GaAs owing to their similar effective carrier masses, but, in reality, it is much lower.²⁵ The carrier mobility can be limited by either intrinsic effects, such as carrier interaction with the lattice (e.g., electron–phonon interactions), or extrinsic effects resulting from material processing (e.g., grain boundaries).²⁵

In the case where grains are large and defects are minimal, intrinsic effects are the limiting factor in carrier transport. In the context of the THz spectroscopy of perovskites, the electron–phonon interactions are one observable that can provide insight into charge transport. More specifically, these interactions include acoustic phonon scattering, interaction via a Fröhlich mechanism, or the formation of large polarons.²⁶ To rationally improve the performance of perovskite materials, it is important to know which of these phenomena is dominant. Because each of these phenomena shows signatures in the THz regime, THz spectroscopy is a valuable tool for gaining such an understanding. For example, photoinduced polaron formation in an all-inorganic perovskite, CsPbBr₃, was reported by Cinquanta et al. Using a combination of TRTS and DFT calculations, they attributed a transient blue shift in the phonon modes to electron–phonon interactions related to polaron formation.²⁷

However, THz spectroscopy can be utilized to enable a much deeper understanding of charge transport through temperature-controlled measurements. A prime example of this can be seen in a report by Zhao et al., studying electron–phonon interactions in a mixed composition perovskite, FA_{0.85}Cs_{0.15}Pb(I_{0.97}Br_{0.03})₃ (FA = formamidinium), or FCIPIB.²⁴ In their work, they performed TRTS as a function of temperature to monitor the transient change in photoconductivity, extracting contributions from both free carriers (Drude–Smith) and phonons (Lorentzian peak shift). By separating these contributions, they were able to model the free-carrier contribution using the Drude–Smith model and extract both the carrier density (N) and the scattering time (τ). In particular, τ was useful for assigning the number of scattering channels in FCIPIB at low temperature (15 K), although at higher temperatures (65 and 285 K), all of the scattering channels were thermally accessible. However, one of the more striking results is their interpretation of N and the change in the phonon spectral weight (i.e., oscillator strength) at

short times (<10 ps) and low temperature (15 K). At long pump–probe delays, third-order recombination is dominant at the pump fluence used, whereas at short times, they observed significant deviations. By comparing both N and the change in phonon spectral weight, or $\Delta(\omega_{\text{pk}}/2\pi)^2$, for both phonon modes, they were able to assign this deviation to the formation and breaking of excitons, resulting in phonon emission and absorption, respectively (Figure 3).²⁴

Whereas Zhao et al.²⁴ probed exciton dynamics indirectly through the number of carriers, THz spectroscopy can also be used to directly probe both the presence and binding energies of excitons. Using ultrafast broadband “multi-THz” spectroscopy, Lan et al. were able to probe exciton dynamics in addition to the charge–phonon correlation in the prototypical perovskite, methylammonium lead iodide (MAPI).¹² Excitons in perovskites typically have binding energies on the order of 3–41 meV (~0.7–10 THz), depending on the composition of the perovskite.^{26,28,29} Whereas the lower end of this energy range is easily accessible, higher energy excitons are outside of the range of typical THz spectrometers. However, their spectrometer used air plasma generation and ABCD, providing a bandwidth of up to ~10 THz (~41 meV), allowing them to directly observe these higher energy exciton transitions and providing direct insight into the process of free carrier generation.

It is important to note that not all materials will have resonant features in the THz regime. However, one can nonetheless extract useful information from THz measurements. One significant challenge encountered when measuring carrier mobilities via THz spectroscopy is the inability to separate the contribution from electrons and holes. Although one can separate electron and hole mobilities using methods such as Hall effect measurements,²⁵ these methods require contacts to be placed on the sample, can alter the material close to the contacts, and are not feasible for all sample geometries, which is especially problematic for nanomaterials. However, this issue can be overcome by combining TRTS with ultrafast transient reflectance (fs-TR) spectroscopy, as reported recently by Zhai et al.³⁰ Using TRTS, they were able to extract the sum of the carrier mobilities ($\sum\mu = \mu_e + \mu_h$) of GaAs and a series of lead-halide perovskites. By incorporating fs-TR measurements, they were able to extract the ambipolar diffusion coefficient (D_{ab}), which is related to the ambipolar mobility (μ_{ab}) by the Einstein

equation and, in turn, can be related to μ_e and μ_h by $1/\mu_{ab} = 1/\mu_e + 1/\mu_h$. This allows for two distinct mobilities to be determined. The only caveat is that the two extracted mobilities are not specific to either electrons or holes and must be assigned using some *a priori* knowledge, such as a calculation or previous literature comparisons of similar materials.³⁰

Metal Oxide Photoelectrodes. THz spectroscopy also has made important contributions to the study of metal oxide photoelectrodes. Metal oxides are often used as photoanodes for oxidation reactions such as water splitting, largely due to their stability under harsh oxidation and pH conditions. However, this important benefit comes at a cost. One such cost is the poor carrier mobility, which impairs the electrode performance because sluggish charge transport limits the rate at which carriers are supplied to the interface to perform water oxidation or other processes. In addition, it inhibits charge separation, making it more likely that free carriers will be lost to recombination. Thus it is imperative to understand the factors that influence carrier mobility. As previously discussed, THz spectroscopy provides insights into a number of processes that are important to carrier mobility, including polaron formation and carrier confinement within nanostructures.

In many metal oxide semiconductors, the key process limiting photoconductivity is the formation of small polarons.³¹ THz spectroscopy has been used to understand this process in emerging metal oxides, most notably in BiVO₄.^{32,33} BiVO₄ is a promising photoanode material due to its small band gap and stability, but its performance is limited by its poor carrier mobility. In two recent studies, THz spectroscopy was used to provide detailed information about the origin of this poor mobility.^{32,33} These studies observed a bleach of the phonon mode at ~ 2 THz and attributed this to the lattice distortion associated with the formation of a polaron. Further computational investigations assigned this phonon mode to a specific lattice vibration between the Bi³⁺ and VO₄³⁻ units. Thus these TRTS measurements were able to help ascribe the limited carrier mobility in BiVO₄ to a specific structural feature. With this information, along with structural studies carried out by other methods,³⁴ it may well be possible to rationally improve the BiVO₄ mobility by means of compositional alteration or other synthetic measures.

One strategy used to mitigate the effects of poor carrier mobility is the use of a nanostructured morphology in which carriers are always close enough to the electrolyte interface that limited mobility is inconsequential. However, nanostructuring is often achieved with agglomerations of nanoparticles, where the grain boundaries separating these nanoparticles pose as obstacles to charge transport. Whereas this might not affect the holes that simply have to reach the surface to carry out water oxidation, the electrons must traverse many of these grain boundaries to reach the electrode back contact. Because of this, changes in grain boundaries have been attributed to significant changes in photoelectrode performance.³⁵ For many systems, the time scale on which a carrier would traverse a single particle is on the picosecond time scale, making THz spectroscopy an attractive technique for studying this behavior.³⁶ Thus the signature of carrier confinement within particles might be observable in the suppression of low-frequency conductivity in the THz regime, as carriers are more likely to encounter grain boundaries at these lower frequencies.³⁷

This can be useful in attributing poor carrier mobility to carrier confinement as opposed to other factors, as shown for α -SnWO₄ by Kölbach et al.³⁷ Here they find that photo-

conductivity in the THz regime is significantly greater than that in the microwave regime, which is consistent with the suppression of photoconductivity at the low frequencies previously discussed. They also demonstrate a decrease in photoconductivity in the microwave region as a function of the particle size, further supporting the carrier confinement interpretation.³⁷ As in the polaron studies, this type of investigation is valuable for the future rational design of photoelectrodes. Here the importance of carrier confinement points toward designs that would enhance interparticle transport as the surest path to increased performance.

The previously discussed work provides a valuable template for future THz contributions to the area of metal oxide photoanodes. For many promising metal oxide photoelectrode candidates, the carrier mobility remains a significant issue,³⁸ and thus detailed investigations of both polarons and carrier confinement will remain important. A number of difficulties present themselves here, however. The lower carrier mobilities found in these materials (e.g., ~ 0.4 cm² V⁻¹ s⁻¹ for BiVO₄)³³ result in low signals in the TRTS experiments discussed here. These low signals require care both in optimizing the instrument as well as in carefully selecting THz generation and detection methods. In addition to achieving the sensitivity required to measure low signals, investigating promising metal oxides will require larger bandwidths than those commonly used in many previous studies. Whereas typical measurements span the range of ~ 0.5 – 2.5 THz, the phonon features that would be useful in studying polaron formation often lie at higher frequencies: For example, phonons of interest in hematite (α -Fe₂O₃) lie as high as ~ 20 THz,³⁹ whereas BiFeO₃ has a phonon mode at ~ 3 THz.⁴⁰ In this regard, new broadband “multi-THz” spectrometers, such as those previously discussed, will be essential to probing these phenomena, and it will be important to evaluate trade-offs between the measurement sensitivity and the bandwidth.

Metal–Organic Frameworks. The classes of materials discussed up to this point are relatively well established, although with many emerging properties still being developed and discovered. We now turn to emerging classes of materials that are less well understood and are at the forefront of materials science and where THz spectroscopy has contributed valuably to early explorations. Metal–organic frameworks (MOFs) are highly ordered, tunable, and porous materials composed of organic linkers interconnecting highly tunable inorganic metal nodes. These properties have proven beneficial for applications in gas separation and storage, chemical sensing, drug delivery, molecular separation, and heterogeneous catalysis. However, partially due to their structural makeup, MOFs tend to be electrically insulating, limiting their efficacy in electrocatalytic and photocatalytic reactions. Yet over the past several years, researchers have overcome this issue by engineering conductive channels into MOF structures.⁴¹ Insulating MOFs have also been modified to impart conductivity by intercalation with redox-active molecules.

THz spectroscopy, including both OPTP and TRTS, is especially relevant to photoconductive MOFs. No other technique has proven capable of measuring subpicosecond photoconductivity in MOFs, which is particularly important to understand them to improve their photoconductivity with further engineering. Alberding et al. published one of the first reports of OPTP on MOFs.⁴² Cu₃(1,3,5-benzenetricarboxylate)₂ (HKUST-1) and Cu[Ni(pyrazine-2,3-dithiolate)₂] are two MOFs that do not exhibit intrinsic photoconductivity. However, when intercalated with redox-active species, 7,7,8,8-

tetracyanoquinodimethane (TCNQ) or iodine, they become photoconductive. In this study, the MOF samples were pressed on top of polyethylene pellets and were measured using OPTP with a 400 nm photoexcitation. $\text{TCNQ}^-@HKUST-1$, $\text{TCNQ}^-@Cu[Ni(pdt)_2]$, and $\text{I}_3^-@Cu[Ni(pdt)_2]$ were all shown to exhibit ultrafast photoconductivity that decayed almost fully within 2 ps.

To explore charge transport in conductive MOFs, one study employed temperature-dependent TRTS.⁴³ These experiments were performed on a semiconducting 2D $\text{Fe}_3(\text{THT})_2(\text{NH}_4)_3$ (THT = 2,3,6,7,10,11-triphenylenehexathiol) free-standing MOF film composed of van der Waals stacked layers. To elucidate the nature of photoconductivity in the sample, the frequency-dependent complex photoconductivity under 800 nm photoexcitation was collected. The frequency-integrated photoconductivity as a function of pump delay (Figure 4a) shows a biphasic decay with a majority of decay occurring on a picosecond time scale.⁴³

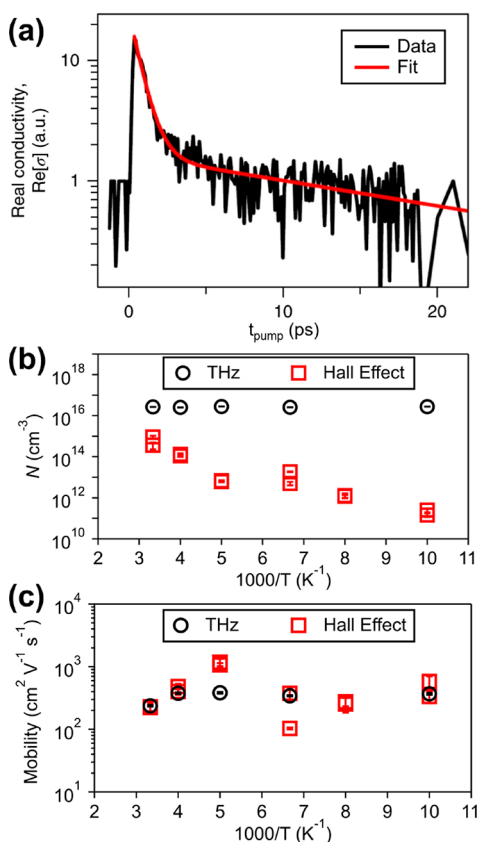


Figure 4. (a) Frequency-integrated photoconductivity as a function of the pump–probe delay for $\text{Fe}_3(\text{THT})_2(\text{NH}_4)_3$ photoexcited with an 800 nm pump pulse at room temperature and a biexponential best fit. Comparison of THz and Hall effect (b) carrier densities (N) and (c) mobilities as a function of temperature. Adapted with permission from ref 43. Copyright 2018 Springer Nature.

TRTS measurements were performed and compared with Hall effect DC measurements as a function of temperature (Figure 4b,c). The Drude fits to THz results were extrapolated to zero frequency for comparison with the DC measurements. The conductivity determined via THz was found to be approximately an order of magnitude larger than the corresponding DC measurement at room temperature. However, the THz mobility and carrier density (black circles, Figure

4b,c) did not decrease as a function of temperature because the carrier density was fixed by the optical pump pulse intensity (i.e., photon flux). In contrast, the carrier density in the Hall experiment decreased exponentially with temperature (red squares, Figure 4b) as the conduction band was thermally depopulated. The carrier mobility was found to be temperature-independent in both measurements, suggesting an impurity carrier scattering mechanism (Figure 4c). Clearly, whereas the comparison with DC measurements yields valuable insight, the photoconductivity information obtained by TRTS is different due to its inclusion of an optical excitation, time resolution, and local sampling, as opposed to the time-averaged long-distance transport in DC measurements. Comparing both experiments therefore allows a more conclusive understanding of the underlying physical mechanism.⁴³

In the previous example, free-standing films of a 2D MOF were measured via TRTS. Such samples are difficult to prepare and limited to few MOFs. Furthermore, they are likely oriented, leading to potential anisotropy concerns that must be addressed during the measurement. Therefore, it is ideal to measure as-prepared polycrystalline MOFs that are randomly oriented in a powder sample to gain isotropic photoconductivity information. In a study from our group, the photoconductivity of the conductive MOF Zn_2TTFTB (TTFTB^{4-} = tetrathiafulvalene tetrabenzoate) was investigated using TRTS in which as-prepared powders were measured.⁴⁴

The OPTP results using 400 nm photoexcitation showed a triexponential decay with an instrument response function (IRF)-limited component (0.6 ps), a 31 ps component, and a long-lived component that accounts for the remaining photoconductivity at the end of the time window (2 ns), the latter being consistent with previous time-resolved microwave conductivity measurements.⁴⁴ The frequency-dependent photoconductivity was fit with the Drude–Smith model, where the carrier scattering time was determined to be 17 fs, which is sufficiently small such that TRTS probes the nonresonant response of free charges and not the Drude plasmon resonance. Furthermore, insight into charge transport within Zn_2TTFTB was gained from the c -parameter, which was determined to be -0.86 , suggesting that charge transport is likely hindered due to grain boundaries or particle size. Insight into the microscopic photoconductivity on a subpicosecond time scale is simply unattainable with any other technique.

Moving forward, the insights gained using THz spectroscopy to investigate MOF photoconductivity will depend on engineering MOFs with larger photoconductivity (to improve signal) or the development of higher sensitivity, ultralow noise spectrometers. Ideally, measurements need to be performed over a wide range of pump fluences to gain further carrier-density-dependent dynamic information.

Beyond photoinduced carrier mobility, TRTS is capable of probing structural dynamics in crystalline MOF materials. Resonant absorption features due to the low-frequency collective motions of several atoms often occur in the THz region of the electromagnetic spectrum and may be useful in understanding the effects of lattice vibrations on charge transport. Temperature-dependent measurements, such as those demonstrated by Dong et al.,⁴³ may be especially useful in this regard. Dynamics have been studied by pressure changes,⁴⁵ temperature effects,⁴⁶ and the effect of gas adsorption on certain resonant absorptions.⁴⁷ These THz-TDS studies highlight the fact that rich structural information can be obtained in MOFs in the THz frequency range, and time-

resolved photoinduced structural dynamics may very well be an important future application of TRTS to MOFs.

2D Materials. 2D materials are typically composed of sheets a few atoms thick that stack through van der Waals forces. There are numerous classes of 2D materials, including graphene, transition metal dichalcogenides (TMDs), and MXenes, with electronic properties ranging from superconducting to insulating and everything in between.⁴⁸ These properties have been taken advantage of in a wide variety of applications such as supercapacitors, batteries, photocatalysts, and photoelectrodes, among others.⁴⁸ For many of these applications, the conductivity and ultrafast photoconductivity are important properties that underlie performance but are currently not fully understood. This makes THz spectroscopy an ideal technique for studying these materials.

Graphene is the prototypical 2D material and has been extensively studied using THz spectroscopy.⁴ A strong message from these studies is that for graphene, as well as other 2D materials, samples produced using different procedures should not be assumed to have similar physical properties as probed via TRTS. Synthetic effects in graphene such as substrate doping have been shown to change the sign of the change in THz transmission,^{49,50} implying increased conductivity after photoexcitation in some cases and decreased conductivity after photoexcitation in others. However, this positions THz spectroscopy as a useful technique for studying these properties of 2D materials as a function of material fabrication parameters.

More recently, THz spectroscopy has been utilized to better understand carrier dynamics in TMDs.⁴ There have been multiple THz studies performed on MoS₂, specifically on the 2H semiconducting phase that is relevant in applications such as batteries and photocatalysts. Docherty et al. used OPTP to study monolayer and trilayer 2H-MoS₂, where the photoexcited carrier lifetime was determined to be three times larger in the trilayer form on an ultrafast time scale even though both samples showed a long-lived photoconductivity signal beyond the measurement time delay range. Monolayer WSe₂ was also studied in this work.⁵¹ Frequency-dependent photoconductivity spectra were measured via TRTS and modeled using a Drude model and a sum of Lorentzian oscillators including excitons and trions. Whereas the Lorentzian features were outside the frequency range of the measurement for 2H-MoS₂, a clear trionic resonance was well-modeled with the Lorentzian model for WSe₂.⁵¹ As with graphene, sample preparation strongly impacts the physical properties of MoS₂. For example, in contrast with the Docherty et al. study, Lui et al. measured decreased conductivity after photoexcitation when using certain preparative procedures.⁵²

MXenes are another class of 2D materials that have been investigated with THz spectroscopy. These materials are made by removing Al from a "MAX" such as Ti₃AlC₂ (where "M" is a metal, sometimes more than one, "A" is Al, and "X" is C or N), resulting in a 2D layered metal carbide or nitride material. Typically, MXenes are multilayer materials, but many can be delaminated to obtain single sheets. As is the case with some other 2D materials, MXenes can demonstrate either metallic or semiconducting properties, suggesting that they may be applicable in energy storage and production systems.⁵⁴ Li et al. recently reported results for Mo-based MXenes, Mo₂TiC₃T_z and Mo₂TiC₂T_z (where T_z represents surface terminations), using THz spectroscopy to study carrier dynamics.⁵³ Ti₃C₂T_z, which is known to have metallic character, yielded greater THz transmission after visible-light photoexcitation, suggesting

reduced carrier mobility after heating of the electron gas, as expected in a metallic conductor. The semiconductor-like Mo₂TiC₃T_z and Mo₂TiC₂T_z showed enhanced photoconductivity upon photoexcitation, and OPTP measurements revealed distinct carrier dynamics, as measured by OPTP before and after an annealing step that decreased the internanosheet distance (Figure 5).⁵³

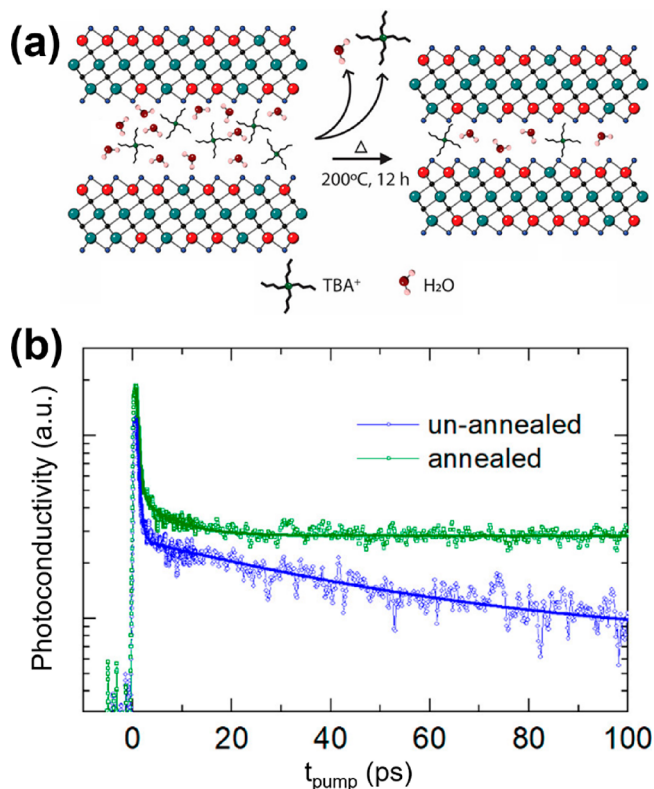


Figure 5. Time-resolved THz spectroscopy of Mo₂TiC₂T_z MXene. (a) Cartoon of the solvent and cation removal effect due to annealing under vacuum, resulting in a change of internanosheet distance. (b) OPTP traces comparing unannealed and annealed samples, showing an increase in the long-time photoconductivity. Adapted with permission from ref 53. Copyright 2020 American Chemical Society.

Frequency-dependent photoconductivity spectra of the unannealed and annealed samples at various time delays were fit using the Drude–Smith model. Here annealing resulted in a less negative c -parameter (i.e., more Drude-like), suggesting higher internanosheet mobility compared with the nonannealed material that has a larger internanosheet distance. Furthermore, by comparing the photoconductivity with the ground state (i.e., dark) conductivity spectrum, it was suggested that ground-state (or intrinsic) conductivity is mainly intranosheet, in contrast with the internanosheet photoconductivity. This work highlights the wealth of knowledge that can be obtained in 2D materials by combining THz-TDS and TRTS, which can be easily performed on the same instrument.

These studies of 2D materials demonstrate the power that THz spectroscopy has in understanding how synthetic conditions can alter the photoconductivity in a material. Furthermore, TRTS may be useful for gaining important mechanistic information regarding interlayer charge transport in 2D material heterostructures formed from different combinations of layered materials due to the weak van der

Waals forces,⁵⁵ a field that certainly will be important for developing tunable materials. In addition, anisotropic measurements may be possible by controlling both the pump polarization and the THz probe polarization as well as the sample orientation to probe specific orientations of the 2D layers in highly ordered samples. Systematic studies aimed at understanding the manner in which synthetic conditions can alter the sign, magnitude, and mechanism of photoconductivity in 2D materials will be instrumental in characterizing the inter-versus intraplane conductivity contributions, among other things. When developing new materials, understanding these contributions is critical toward the effective application of 2D materials in devices.

CONCLUSIONS AND OUTLOOK

THz spectroscopy has proven to be a powerful tool in understanding the photoelectrical properties of emerging materials. Over the past few decades, THz spectroscopy has matured into a technique that is accessible to new users, yet it is still making improvements at the cutting edge of THz science. For example, recent work by Tarekegne et al. studied THz nonlinearity in 4H-SiC using 2D THz spectroscopy (i.e., THz-pump, THz-probe), which is a state-of-the-art technique analogous to 2D-IR spectroscopy that may have applications in studying other emerging materials.¹⁶ The insights provided by THz measurements provide mechanistic information that is unobtainable using other methodologies. In addition, the contact-free nature of the technique and the flexibility in sample geometry make this technique especially useful for emerging materials. Methods for sample preparation range from powders pressed into pellets,¹¹ to thin films,⁵⁶ to suspensions of small sample quantities in Nafion,⁶ demonstrating that THz spectroscopy is applicable to the study of a diverse array of materials.

It is clear that investigating the next generation of materials will require two advancements in THz technologies. The first of these is the development of large bandwidth “multi-THz” spectrometers to probe high-frequency resonant and dielectric phenomena that may be limiting charge transport in emerging materials. For example, even with established techniques such as ABCD, there exist other broadband detection methods such as solid-state biased coherent detection (ss-BCD),⁵⁷ which is already commercially available and yields a bandwidth out to ~10 THz. Second, the development of ultrahigh SNR and dynamic range spectrometers will be essential for measuring low-signal materials that are at the forefront of materials science and will allow for full 2D TRTS measurements to be achievable in a reasonable time frame.

In addition to highlighting technical advances, it is essential to stress that collaboration between materials scientists, spectroscopists, and theoreticians will become increasingly important.⁵⁸ In such a collaborative framework, experts in THz spectroscopy can study materials at the forefront of materials science using state-of-the-art methodology and accurately describe their data in collaboration with theoreticians. Much of the work described here was the result of collaborative efforts, and the resulting insights—whether it is how electron–phonon interactions affect charge transport or simply how the material mobility changes with composition—would not have been possible without such collaborations. Moving forward, it is crucial that we maintain such a collaborative network of materials scientists, spectroscopists (THz or otherwise), and theoreticians to greatly advance the development of the next generation of materials.

AUTHOR INFORMATION

Corresponding Author

Jacob A. Spies — Department of Chemistry and Energy Sciences Institute, Yale University, New Haven, Connecticut 06520, United States; orcid.org/0000-0002-0148-4823; Email: jacob.spies@aya.yale.edu

Authors

Jens Neu — Department of Molecular Biophysics and Biochemistry and Microbial Sciences Institute, Yale University, New Haven, Connecticut 06520, United States; orcid.org/0000-0002-1054-0444

Uriel T. Tayvah — Department of Chemistry and Energy Sciences Institute, Yale University, New Haven, Connecticut 06520, United States; orcid.org/0000-0002-2759-131X

Matt D. Capobianco — Department of Chemistry and Energy Sciences Institute, Yale University, New Haven, Connecticut 06520, United States; orcid.org/0000-0002-1325-8882

Brian Pattengale — Department of Chemistry and Energy Sciences Institute, Yale University, New Haven, Connecticut 06520, United States; orcid.org/0000-0002-1749-4081

Sarah Ostresh — Department of Chemistry and Energy Sciences Institute, Yale University, New Haven, Connecticut 06520, United States; orcid.org/0000-0002-8000-476X

§Charles A. Schmuttenmaer — Department of Chemistry and Energy Sciences Institute, Yale University, New Haven, Connecticut 06520, United States; orcid.org/0000-0001-9992-8578

Complete contact information is available at:
<https://pubs.acs.org/10.1021/acs.jpcc.0c06344>

Notes

The authors declare no competing financial interest.
§C.A.S.: Deceased: July 26, 2020.

Biographies



Jacob A. Spies (back row, left) earned his B.S. in Chemistry from The Pennsylvania State University in 2016, where he studied charge transport control in water splitting photoelectrochemical cells with Prof. Thomas Mallouk. Jacob is currently a Ph.D. candidate in Chemistry at Yale University under the supervision of Prof. Charles Schmuttenmaer. His research interests focus on using a combination of time-resolved spectroscopic techniques to study charge transport dynamics in solar materials and applications of THz spectroscopy to biophysics.

Dr. Jens Neu (front row, second from right) received his Diploma degree in experimental physics from TU Kaiserslautern in 2010 for his

research on spatially resolved THz near- and far-field spectroscopy. He then joined the research group of Prof. Marco Rahm at TU Kaiserslautern, where he worked toward adaptive silicon-based metamaterials for the THz spectral range and received his Ph.D. degree in experimental physics in 2016. After graduation, he joined the Department of Chemistry at Yale University as a postdoctoral associate with Prof. Charles Schmuttenmaer. His research interests include THz spectroscopy, metamaterials for THz applications, biophysics, and solar cell research. His expertise in this field includes numerical simulations as well as experimental characterization techniques.

Uriel T. Tayvah (front row, left) received his B.A. in Chemistry from Princeton University, where he studied electrochemistry and computational chemistry under Prof. Andrew Bocarsly and Prof. Annabella Selloni. He is currently a Ph.D. candidate at Yale University working under the supervision of Prof. Charles Schmuttenmaer, focusing on using THz spectroscopy to study charge transport in materials for solar fuels.

Matt D. Capobianco (back row, right) received his B.A. in Chemistry and B.S. in Applied Mathematics from Marist College while performing research in computational chemistry with Prof. John Galbraith. Upon graduation in 2018, he continued his education at Yale University, where he is now a Ph.D. candidate in Chemistry under the supervision of Prof. Charles Schmuttenmaer, where he uses THz spectroscopy to study carrier dynamics in 2D materials.

Dr. Brian Pattengale (back row, center) is a postdoctoral associate in the group of Prof. Charles Schmuttenmaer in the Energy Sciences Institute and Department of Chemistry at Yale University. He received his Ph.D. from Marquette University working with Prof. Jier Huang and received his B.S. in Biochemistry from Carroll University. His research interests are directed to studying photoinduced processes in emerging materials using ultrafast time-resolved spectroscopic techniques. His current research involves applying time-resolved THz spectroscopy to obtain photoconductivity information in metal–organic frameworks and 2D materials relevant to photocatalysis and solar fuels.

Sarah Ostresh (front row, second from left) received her B.S. in Chemistry from the University of Southern California in 2017. While there, she conducted research with Prof. Jahan Dawlaty, where she became interested in ultrafast spectroscopy. She is currently pursuing her Ph.D. at Yale University under the supervision of Prof. Charles Schmuttenmaer. Her research focuses on using THz spectroscopy to study charge transport in nanostructured materials for energy conversion.

Prof. Charles A. Schmuttenmaer (front row, right) hails from Oak Park, Illinois, just outside of Chicago. He received his B.S. in Chemistry in 1985 from the University of Illinois, Urbana–Champaign, and then went on to the University of California, Berkeley for his Ph.D. research, which was awarded in 1991. After completing his postdoctoral studies at the University of Rochester, he joined the faculty at Yale in 1994. The primary focus of his research is THz spectroscopy of nanomaterials that will play a role in artificial photosynthesis; molecular crystals; and, more recently, metal–organic frameworks and 2D materials. He is a fellow of the American Association for the Advancement of Science, the American Physical Society, and the Royal Society of Chemistry.

ACKNOWLEDGMENTS

This work was supported by the U.S. Department of Energy, Office of Science, Office of Basic Energy Sciences (DE-FG02-07ER15909) as well as by a generous donation from the TomKat Foundation. J.A.S. acknowledges support from the Onsager Graduate Research Fellowship in Chemistry. U.T.T. acknowledges the support of the National Science Foundation

Graduate Research Fellowship (DGE-1752134). The authors would like to thank Dr. Matthew C. Beard for his helpful discussions.

REFERENCES

- (1) Sze, S. M.; Ng, K. K. *Physics of Semiconductor Devices*; John Wiley & Sons, Inc.: Hoboken, NJ, 2006.
- (2) Neu, J.; Schmuttenmaer, C. A. Tutorial: An introduction to terahertz time domain spectroscopy (THz-TDS). *J. Appl. Phys.* **2018**, *124*, 231101.
- (3) Zhao, D.; Chia, E. E. M. Free Carrier, Exciton, and Phonon Dynamics in Lead-Halide Perovskites Studied with Ultrafast Terahertz Spectroscopy. *Adv. Opt. Mater.* **2020**, *8*, 1900783.
- (4) Han, P.; Wang, X.; Zhang, Y. Time-Resolved Terahertz Spectroscopy Studies on 2D Van der Waals Materials. *Adv. Opt. Mater.* **2020**, *8*, 1900533.
- (5) Beard, M. C.; Turner, G. M.; Schmuttenmaer, C. A. Transient photoconductivity in GaAs as measured by time-resolved terahertz spectroscopy. *Phys. Rev. B: Condens. Matter Mater. Phys.* **2000**, *62*, 15764–15777.
- (6) Spies, J. A.; Hilibrand, M. J.; Neu, J.; Ostresh, S.; Swierk, J. R.; Schmuttenmaer, C. A. Suspensions of Semiconducting Nanoparticles in Nafion for Transient Spectroscopy and Terahertz Photoconductivity Measurements. *Anal. Chem.* **2020**, *92*, 4187–4192.
- (7) Neu, J.; Rahm, M. Terahertz time domain spectroscopy for carrier lifetime mapping in the picosecond to microsecond regime. *Opt. Express* **2015**, *23*, 12900–12909.
- (8) Neu, J.; Regan, K. P.; Swierk, J. R.; Schmuttenmaer, C. A. Applicability of the thin-film approximation in terahertz photoconductivity measurements. *Appl. Phys. Lett.* **2018**, *113*, 233901.
- (9) La-o-vorakiat, C.; Cheng, L.; Salim, T.; Marcus, R. A.; Michel-Beyerle, M.-E.; Lam, Y. M.; Chia, E. E. M. Phonon features in terahertz photoconductivity spectra due to data analysis artifact: A case study on organometallic halide perovskites. *Appl. Phys. Lett.* **2017**, *110*, 123901.
- (10) Richter, C.; Schmuttenmaer, C. A. Exciton-like trap states limit electron mobility in TiO₂ nanotubes. *Nat. Nanotechnol.* **2010**, *5*, 769–772.
- (11) Neu, J.; Stone, E. A.; Spies, J. A.; Storch, G.; Hatano, A. S.; Mercado, B. Q.; Miller, S. J.; Schmuttenmaer, C. A. Terahertz Spectroscopy of Tetrameric Peptides. *J. Phys. Chem. Lett.* **2019**, *10*, 2624–2628.
- (12) Lan, Y.; Tao, X.; Kong, X.; He, Y.; Zheng, X.; Sutton, M.; Kanatzidis, M. G.; Guo, H.; Cooke, D. G. Coherent charge-phonon correlations and exciton dynamics in orthorhombic CH₃NH₃PbI₃ measured by ultrafast multi-THz spectroscopy. *J. Chem. Phys.* **2019**, *151*, 214201.
- (13) Aoki, K.; Savolainen, J.; Havenith, M. Broadband terahertz pulse generation by optical rectification in GaP crystals. *Appl. Phys. Lett.* **2017**, *110*, 201103.
- (14) Ilyakov, I. E.; Kitaeva, G. K.; Shishkin, B. V.; Akhmedzhanov, R. A. The use of DSTMS crystal for broadband terahertz electro-optic sampling based on laser pulse amplitude changes. *Laser Phys. Lett.* **2018**, *15*, 125401.
- (15) Zhang, Y.; Zhang, X.; Li, S.; Gu, J.; Li, Y.; Tian, Z.; Ouyang, C.; He, M.; Han, J.; Zhang, W. A Broadband THz-TDS System Based on DSTMS Emitter and LTG InGaAs/InAlAs Photoconductive Antenna Detector. *Sci. Rep.* **2016**, *6*, 26949.
- (16) Tarekegne, A. T.; Kaltenecker, K. J.; Klarskov, P.; Iwaszczuk, K.; Lu, W.; Ou, H.; Norrman, K.; Jepsen, P. U. Subcycle Nonlinear Response of Doped 4H Silicon Carbide Revealed by Two-Dimensional Terahertz Spectroscopy. *ACS Photonics* **2020**, *7*, 221–231.
- (17) Lu, X.; Zhang, X. C. Balanced terahertz wave air-biased-coherent-detection. *Appl. Phys. Lett.* **2011**, *98*, 151111.
- (18) Seifert, T.; Jaiswal, S.; Martens, U.; Hannegan, J.; Braun, L.; Maldonado, P.; Freimuth, F.; Kronenberg, A.; Henrizi, J.; Radu, I.; Beaupaire, E.; Mokrousov, Y.; Oppeneer, P. M.; Jourdan, M.; Jakob, G.; Turchinovich, D.; Hayden, L. M.; Wolf, M.; Müntenberg, M.; Kläui,

M.; Kampfrath, T. Efficient metallic spintronic emitters of ultra-broadband terahertz radiation. *Nat. Photonics* **2016**, *10*, 483–488.

(19) Glover, R. E.; Tinkham, M. Conductivity of Superconducting Films for Photon Energies between 0.3 and 40 kT_c. *Phys. Rev.* **1957**, *108*, 243–256.

(20) GitHub Repository. <https://github.com/YaleTHz>; accessed August 18, 2020.

(21) Lloyd-Hughes, J.; Jeon, T.-I. A Review of the Terahertz Conductivity of Bulk and Nano-Materials. *J. Infrared, Millimeter, Terahertz Waves* **2012**, *33*, 871–925.

(22) Smith, N. Classical generalization of the Drude formula for the optical conductivity. *Phys. Rev. B: Condens. Matter Mater. Phys.* **2001**, *64*, 155106.

(23) Cocker, T. L.; Baillie, D.; Buruma, M.; Titova, L. V.; Sydora, R. D.; Marsiglio, F.; Hegmann, F. A. Microscopic origin of the Drude-Smith model. *Phys. Rev. B: Condens. Matter Mater. Phys.* **2017**, *96*, 205439.

(24) Zhao, D.; Hu, H.; Haselsberger, R.; Marcus, R. A.; Michel-Beyerle, M. E.; Lam, Y. M.; Zhu, J. X.; La-o-vorakiat, C.; Beard, M. C.; Chia, E. E. M. Monitoring Electron-Phonon Interactions in Lead Halide Perovskites Using Time-Resolved THz Spectroscopy. *ACS Nano* **2019**, *13*, 8826–8835.

(25) Herz, L. M. Charge-Carrier Mobilities in Metal Halide Perovskites: Fundamental Mechanisms and Limits. *ACS Energy Lett.* **2017**, *2*, 1539–1548.

(26) Ghosh, D.; Welch, E.; Neukirch, A. J.; Zakhidov, A.; Tretiak, S. Polarons in Halide Perovskites: A Perspective. *J. Phys. Chem. Lett.* **2020**, *11*, 3271–3286.

(27) Cinquanta, E.; Meggiolaro, D.; Motti, S. G.; Gandini, M.; Alcocer, M. J. P.; Akkerman, Q. A.; Vozzi, C.; Manna, L.; De Angelis, F.; Petrozza, A.; Stagira, S. Ultrafast THz Probe of Photoinduced Polarons in Lead-Halide Perovskites. *Phys. Rev. Lett.* **2019**, *122*, 166601.

(28) Milot, R. L.; Klug, M. T.; Davies, C. L.; Wang, Z.; Kraus, H.; Snaith, H. J.; Johnston, M. B.; Herz, L. M. The Effects of Doping Density and Temperature on the Optoelectronic Properties of Formamidinium Tin Triiodide Thin Films. *Adv. Mater.* **2018**, *30*, 1804506.

(29) Davies, C. L.; Borchert, J.; Xia, C. Q.; Milot, R. L.; Kraus, H.; Johnston, M. B.; Herz, L. M. Impact of the Organic Cation on the Optoelectronic Properties of Formamidinium Lead Triiodide. *J. Phys. Chem. Lett.* **2018**, *9*, 4502–4511.

(30) Zhai, Y.; Wang, K.; Zhang, F.; Xiao, C.; Rose, A. H.; Zhu, K.; Beard, M. C. Individual Electron and Hole Mobilities in Lead-Halide Perovskites Revealed by Noncontact Methods. *ACS Energy Lett.* **2020**, *5*, 47–55.

(31) Rettie, A. J.; Chemelewski, W. D.; Emin, D.; Mullins, C. B. Unravelling Small-Polaron Transport in Metal Oxide Photoelectrodes. *J. Phys. Chem. Lett.* **2016**, *7*, 471–479.

(32) Butler, K. T.; Dringoli, B. J.; Zhou, L.; Rao, P. M.; Walsh, A.; Titova, L. V. Ultrafast carrier dynamics in BiVO₄ thin film photoanode material: interplay between free carriers, trapped carriers and low-frequency lattice vibrations. *J. Mater. Chem. A* **2016**, *4*, 18516–18523.

(33) Ziwrtsch, M.; Müller, S.; Hempel, H.; Unold, T.; Abdi, F. F.; van de Krol, R.; Friedrich, D.; Eichberger, R. Direct Time-Resolved Observation of Carrier Trapping and Polaron Conductivity in BiVO₄. *ACS Energy Lett.* **2016**, *1*, 888–894.

(34) Pattengale, B.; Ludwig, J.; Huang, J. Atomic Insight into the W-Doping Effect on Carrier Dynamics and Photoelectrochemical Properties of BiVO₄ Photoanodes. *J. Phys. Chem. C* **2016**, *120*, 1421–1427.

(35) Warren, S. C.; Voitchovsky, K.; Dotan, H.; Leroy, C. M.; Cornuz, M.; Stellacci, F.; Hebert, C.; Rothschild, A.; Gratzel, M. Identifying champion nanostructures for solar water-splitting. *Nat. Mater.* **2013**, *12*, 842–849.

(36) Titova, L. V.; Cocker, T. L.; Cooke, D. G.; Wang, X.; Meldrum, A.; Hegmann, F. A. Ultrafast percolative transport dynamics in silicon nanocrystal films. *Phys. Rev. B: Condens. Matter Mater. Phys.* **2011**, *83*, 085403.

(37) Kölbach, M.; Hempel, H.; Harbauer, K.; Schleuning, M.; Petsiuk, A.; Höflich, K.; Deinhart, V.; Friedrich, D.; Eichberger, R.; Abdi, F. F.; van de Krol, R. Grain Boundaries Limit the Charge Carrier Transport in Pulsed Laser Deposited α -SnWO₄ Thin Film Photoabsorbers. *ACS Appl. Energy Mater.* **2020**, *3*, 4320–4330.

(38) Lee, D. K.; Lee, D.; Lumley, M. A.; Choi, K. S. Progress on ternary oxide-based photoanodes for use in photoelectrochemical cells for solar water splitting. *Chem. Soc. Rev.* **2019**, *48*, 2126–2157.

(39) Kay, A.; Fiegenbaum-Raz, M.; Müller, S.; Eichberger, R.; Dotan, H.; de Krol, R.; Abdi, F. F.; Rothschild, A.; Friedrich, D.; Grave, D. A. Effect of Doping and Excitation Wavelength on Charge Carrier Dynamics in Hematite by Time-Resolved Microwave and Terahertz Photoconductivity. *Adv. Funct. Mater.* **2020**, *30*, 1901590.

(40) Chen, P.; Xu, X.; Koenigsmann, C.; Santulli, A. C.; Wong, S. S.; Musfeldt, J. L. Size-dependent infrared phonon modes and ferroelectric phase transition in BiFeO₃ nanoparticles. *Nano Lett.* **2010**, *10*, 4526–32.

(41) Xie, L. S.; Skorupskii, G.; Dinca, M. Electrically Conductive Metal-Organic Frameworks. *Chem. Rev.* **2020**, *120* (16), 8536–8580.

(42) Alberding, B. G.; Heilweil, E. J. Time-resolved terahertz spectroscopy of electrically conductive metal-organic frameworks doped with redox active species. *Proc. SPIE* **2015**, 9567, 95671L.

(43) Dong, R.; Han, P.; Arora, H.; Ballabio, M.; Karakus, M.; Zhang, Z.; Shekhar, C.; Adler, P.; Petkov, P. S.; Erbe, A.; Mannsfeld, S. C. B.; Felser, C.; Heine, T.; Bonn, M.; Feng, X.; Canovas, E. High-mobility band-like charge transport in a semiconducting two-dimensional metal-organic framework. *Nat. Mater.* **2018**, *17*, 1027–1032.

(44) Narayan, T. C.; Miyakai, T.; Seki, S.; Dinca, M. High charge mobility in a tetrathiafulvalene-based microporous metal-organic framework. *J. Am. Chem. Soc.* **2012**, *134*, 12932–12935.

(45) Zhang, W.; Maul, J.; Vulpe, D.; Moghadam, P. Z.; Fairen-Jimenez, D.; Mittleman, D. M.; Zeitler, J. A.; Erba, A.; Ruggiero, M. T. Probing the Mechanochemistry of Metal–Organic Frameworks with Low-Frequency Vibrational Spectroscopy. *J. Phys. Chem. C* **2018**, *122*, 27442–27450.

(46) Li, Q.; Zaczek, A. J.; Korter, T. M.; Zeitler, J. A.; Ruggiero, M. T. Methyl-rotation dynamics in metal-organic frameworks probed with terahertz spectroscopy. *Chem. Commun.* **2018**, *54*, 5776–5779.

(47) Tanno, T.; Watanabe, Y.; Umeno, K.; Matsuoka, A.; Matsumura, H.; Odaka, M.; Ogawa, N. In Situ Observation of Gas Adsorption onto ZIF-8 Using Terahertz Waves. *J. Phys. Chem. C* **2017**, *121*, 17921–17924.

(48) Hynek, D. J.; Pondick, J. V.; Cha, J. J. The development of 2D materials for electrochemical energy applications: A mechanistic approach. *APL Mater.* **2019**, *7*, 030902.

(49) Choi, H.; Borondics, F.; Siegel, D. A.; Zhou, S. Y.; Martin, M. C.; Lanzara, A.; Kaindl, R. A. Broadband electromagnetic response and ultrafast dynamics of few-layer epitaxial graphene. *Appl. Phys. Lett.* **2009**, *94*, 172102.

(50) Fu, M.; Wang, X.; Ye, J.; Feng, S.; Sun, W.; Han, P.; Zhang, Y. Strong negative terahertz photoconductivity in photoexcited graphene. *Opt. Commun.* **2018**, *406*, 234–238.

(51) Docherty, C. J.; Parkinson, P.; Joyce, H. J.; Chiu, M.-H.; Chen, C.-H.; Lee, M.-Y.; Li, L.-J.; Herz, L. M.; Johnston, M. B. Ultrafast Transient Terahertz Conductivity of Monolayer MoS₂ and WSe₂ Grown by Chemical Vapor Deposition. *ACS Nano* **2014**, *8*, 11147–11153.

(52) Lui, C. H.; Frenzel, A. J.; Pilon, D. V.; Lee, Y. H.; Ling, X.; Akselrod, G. M.; Kong, J.; Gedik, N. Trion-induced negative photoconductivity in monolayer MoS₂. *Phys. Rev. Lett.* **2014**, *113*, 166801.

(53) Li, G.; Natu, V.; Shi, T.; Barsoum, M. W.; Titova, L. V. Two-Dimensional MXenes Mo₂Ti₂C₃T_z and Mo₂TiC₂T_z: Microscopic Conductivity and Dynamics of Photoexcited Carriers. *ACS Appl. Energy Mater.* **2020**, *3*, 1530–1539.

(54) Pang, J.; Mendes, R. G.; Bachmatiuk, A.; Zhao, L.; Ta, H. Q.; Gemming, T.; Liu, H.; Liu, Z.; Rummeli, M. H. Applications of 2D MXenes in energy conversion and storage systems. *Chem. Soc. Rev.* **2019**, *48*, 72–133.

(55) Das, P.; Fu, Q.; Bao, X.; Wu, Z.-S. Recent advances in the preparation, characterization, and applications of two-dimensional heterostructures for energy storage and conversion. *J. Mater. Chem. A* **2018**, *6*, 21747–21784.

(56) Neu, J.; Ostresh, S.; Regan, K. P.; Spies, J. A.; Schmittenmaer, C. A. Influence of Dye Sensitizers on Charge Dynamics in SnO₂ Nanoparticles Probed with THz Spectroscopy. *J. Phys. Chem. C* **2020**, *124*, 3482–3488.

(57) Tomasino, A.; Mazhorova, A.; Clerici, M.; Peccianti, M.; Ho, S.-P.; Jestin, Y.; Pasquazi, A.; Markov, A.; Jin, X.; Piccoli, R.; Delprat, S.; Chaker, M.; Busacca, A.; Ali, J.; Razzari, L.; Morandotti, R. Solid-state-biased coherent detection of ultra-broadband terahertz pulses. *Optica* **2017**, *4*, 1358.

(58) Spies, J. A.; Perets, E. A.; Fisher, K. J.; Rudshiteyn, B.; Batista, V. S.; Brudvig, G. W.; Schmittenmaer, C. A. Collaboration between experiment and theory in solar fuels research. *Chem. Soc. Rev.* **2019**, *48*, 1865–1873.